blood

American Society of Hematology
2021 L Street NW, Suite 900,
Washington, DC 20036
Phone: 202-776-0544 | Fax 202-776-0545
editorial@hematology.org

# Mitochondrial tRNA pseudouridylation governs erythropoiesis

Tracking no: BLD-2023-022004R2

Bichen Wang (State Key Laboratory of Experimental Hematology, Institute of Hematology and Blood Diseases Hospital, Chinese Academy of Medical Sciences and Peking Union Medical College, China) Deyang Shi (State Key Laboratory of Experimental Hematology, Institute of Hematology and Blood Diseases Hospital, Chinese Academy of Medical Sciences and Peking Union Medical College, China) Shuang Yang (State Key Laboratory of Experimental Hematology, National Clinical Research Center for Blood Diseases, Institute of Hematology & Blood Diseases Hospital, Chinese Academy of Medical Sciences & Peking Union Medical College, China) Yu lian (Shanxi Bethune Hospital Department of Hematology, China) Haoyuan Li (State Key Laboratory of Experimental Hematology, Institute of Hematology and Blood Diseases Hospital, Chinese Academy of Medical Sciences and Peking Union Medical College, China) Mutian Cao (State Key Laboratory of Experimental Hematology, National Clinical Research Center for Blood Diseases, Institute of Hematology & Blood Diseases Hospital, Chinese Academy of Medical Sciences & Peking Union Medical College, China) Yifei He (State Key Laboratory of Experimental Hematology, Institute of Hematology and Blood Diseases Hospital, Chinese Academy of Medical Sciences and Peking Union Medical College, China) Lele Zhang (State Key Laboratory of Experimental Hematology, National Clinical Research Center for Blood Diseases, Haihe Laboratory of Cell Ecosystem, PUMC Department of Stem Cell and Regenerative Medicine, CAMS Key Laboratory of Gene Therapy for Blood Diseases, Institute of Hematology & Blood Diseases Hospital, Chinese Academy of Medical Sciences & Peking Union Medical College, China) Chen Qiu (State Key Laboratory of Experimental Hematology, Institute of Hematology and Blood Diseases Hospital, Chinese Academy of Medical Sciences and Peking Union Medical College, China) Tong Liu (State Key Laboratory of Experimental Hematology, National Clinical Research Center for Blood Diseases, Institute of Hematology & Blood Diseases Hospital, Chinese Academy of Medical Sciences & Peking Union Medical College, China) Wei Wen (Institute of Hematology and Blood Disease Hospital, China) Yuanwu Ma (Key Laboratory of Human Disease Comparative Medicine, National Health Commission of China (NHC), AND Beijing Engineering Research Center for Experimental Animal Models of Human Critical Diseases, Institute of Laboratory Animal Science, Chinese Academy of Medical Sciences, Peking Union Medicine College, China) Lei Shi (Key Laboratory of Breast Cancer Prevention and Therapy (Ministry of Education), Haihe Laboratory of Cell Ecosystem, Department of Biochemistry and Molecular Biology, School of Basic Medical Sciences, Tianjin Medical University Cancer Institute and Hospital, Tianjin Medical University, China) Tao Cheng (State Key Laboratory of Experimental Hematology, National Clinical Research Center for Blood Diseases, Institute of Hematology & Blood Diseases Hospital, Chinese Academy of Medical Sciences & Peking, China) Lihong Shi (Institute of Hematology & Blood Diseases Hospital, Chinese academy of medical sciences, China) Weiping Yuan (State Key Laboratory of Experimental Hematology, National Clinical Research Center for Blood Diseases, Haihe Laboratory of Cell Ecosystem, Institute of Hematology & Blood Diseases Hospital, Chinese Academy of Medical Sciences & Peking Union Medical College, China) Yajing Chu (State Key Laboratory of Experimental Hematology, National Clinical Research Center for Blood Diseases, Institute of Hematology & Blood Diseases Hospital, Chinese Academy of Medical Sciences & Peking Union Medical College, China) Jun Shi (State Key Laboratory of Experimental Hematology, National Clinical Research Center for Blood Diseases, Haihe Laboratory of Cell Ecosystem, Institute of Hematology & Blood Diseases Hospital, Chinese Academy of Medical Sciences and Peking Union Medical College; Tianjin Institutes of Health Science; Regenerative Medicine Clinic & Red Blood Cell Diseases, Institute of Hematology & Blood Diseases Hospital, Chinese Academy of Medical Sciences and Peking Union Medical College, China)

**Abstract:**
Pseudouridine is the most prevalent RNA modification, and its aberrant function is implicated in various human diseases. However, the specific impact of pseudouridylation on hematopoiesis remains poorly understood. In this study, we investigated the role of tRNA pseudouridylation in erythropoiesis and its association with mitochondrial myopathy, lactic acidosis, and sideroblastic anemia syndrome (MLASA) pathogenesis. By utilizing patient-specific induced pluripotent stem cells (iPSCs) carrying a genetic PUS1 mutation and a corresponding mutant mouse model, we demonstrated impaired erythropoiesis in MLASA iPSCs and anemia in the MLASA mouse model. Both MLASA iPSCs and mouse erythroblasts exhibited compromised mitochondrial function and impaired protein synthesis. Mechanistically, we revealed that PUS1 deficiency resulted in reduced mitochondrial tRNA levels due to pseudouridylation loss, leading to aberrant mitochondrial translation. Screening of mitochondrial supplements aimed at enhancing respiration or heme synthesis showed limited effect in promoting erythroid differentiation. Interestingly, the mTOR inhibitor rapamycin facilitated erythroid differentiation in MLASA-iPSCs by suppressing mTOR signaling and protein synthesis, and consistent results were observed in the MLASA mouse model. Importantly, rapamycin treatment effectively ameliorated anemia phenotypes in the MLASA patient. Our findings provide novel insights into the crucial role of mitochondrial tRNA pseudouridylation in governing erythropoiesis and present potential therapeutic strategies for anemia patients facing challenges related to protein translation. -

**Conflict of interest:** No COI declared

**COI notes:**

**Preprint server:** No;

**Author contributions and disclosures:** JS, YJC and WPY conceived the project, supervised the research and revised the paper. BCW, DYS, SY, YL and YJC designed and performed most of the experiments, wrote and revised the paper. HYL, MTC, YFH, LLZ, CQ, TL and WW assisted with experiments and data analysis, YWM, LS, TC and LHS contributed to the research design and paper discussion.

**Non-author contributions and disclosures:** No;

**Agreement to Share Publication-Related Data and Data Sharing Statement:** Our high-throughput datasets were deposited to public GSA-human repository with the accession number [HRA003814]. Correspondence to: chuyajing@ihcams.ac.cn and shijun@ihcams.ac.cn.

**Clinical trial registration information (if any):**

# Mitochondrial tRNA pseudouridylation governs erythropoiesis

Bichen Wang[1,2 #], Deyang Shi[1,2 #], Shuang Yang[1,2 #], Yu Lian[1,3,4 #], Haoyuan Li[1,2], Mutian Cao[1,2], Yifei He[1,2], Lele Zhang[1,2,3], Chen Qiu[1,2], Tong Liu[1,2], Wei Wen[1,2], Yuanwu Ma[5], Lei Shi[6], Tao Cheng[1,2], Lihong Shi[1,2], Weiping Yuan[1,2 *], Yajing Chu[1,2 *] and Jun Shi[1,2,3 *]

[1]State Key Laboratory of Experimental Hematology, National Clinical Research Center for Blood Diseases, Haihe Laboratory of Cell Ecosystem, Institute of Hematology & Blood Diseases Hospital, Chinese Academy of Medical Sciences and Peking Union Medical College, Tianjin, 300020, China.
[2]Tianjin Institutes of Health Science, Tianjin 301600, China.
[3]Regenerative Medicine Clinic & Red Blood Cell Diseases, Institute of Hematology & Blood Diseases Hospital, Chinese Academy of Medical Sciences and Peking Union Medical College, Tianjin, 300020, China.
[4]Department of Hematology, Shanxi Bethune Hospital, Shanxi Academy of Medical Sciences, Tongji Shanxi Hospital, Third Hospital of Shanxi Medical University, Taiyuan, 030032, China
[5]Key Laboratory of Human Disease Comparative Medicine, National Health Commission of China (NHC), Institute of Laboratory Animal Science, Peking Union Medicine College, Chinese Academy of Medical Sciences, Beijing 100021, China.
[6]Key Laboratory of Breast Cancer Prevention and Therapy (Ministry of Education), Haihe Laboratory of Cell Ecosystem, Department of Biochemistry and Molecular Biology, School of Basic Medical Sciences, Tianjin Medical University Cancer Institute and Hospital, Tianjin Medical University, Tianjin, China.

[#]These authors contributed equally to this work.
[*]Correspondence to: shijun@ihcams.ac.cn (J. Shi), chuyajing@ihcams.ac.cn (Y. Chu), or wpyuan@ihcams.ac.cn (W. Yuan)

Our high-throughput datasets were deposited to public GSA-human repository with the accession number [HRA003814]. Correspondence to: chuyajing@ihcams.ac.cn and shijun@ihcams.ac.cn.

Abstract: 208 words
Text: 3999 words

35 Figures: 7

36 References: 48

**Key points：**

- The deficiency of Ψ in mt-tRNAs due to *PUS1* mutation contributes to impaired mitochondrial function and anemia in an MLASA patient
- The mTOR inhibitor rapamycin shows promise as a therapeutic approach for MLASA-associated anemia


**Abstract**

Pseudouridine is the most prevalent RNA modification, and its aberrant function is implicated in various human diseases. However, the specific impact of pseudouridylation on hematopoiesis remains poorly understood. In this study, we investigated the role of tRNA pseudouridylation in erythropoiesis and its association with mitochondrial myopathy, lactic acidosis, and sideroblastic anemia syndrome (MLASA) pathogenesis. By utilizing patient-specific induced pluripotent stem cells (iPSCs) carrying a genetic PUS1 mutation and a corresponding mutant mouse model, we demonstrated impaired erythropoiesis in MLASA iPSCs and anemia in the MLASA mouse model. Both MLASA iPSCs and mouse erythroblasts exhibited compromised mitochondrial function and impaired protein synthesis. Mechanistically, we revealed that PUS1 deficiency resulted in reduced mitochondrial tRNA levels due to pseudouridylation loss, leading to aberrant mitochondrial translation. Screening of mitochondrial supplements aimed at enhancing respiration or heme synthesis showed limited effect in promoting erythroid differentiation. Interestingly, the mTOR inhibitor rapamycin facilitated erythroid differentiation in MLASA-iPSCs by suppressing mTOR signaling and protein synthesis, and consistent results were observed in the MLASA mouse model. Importantly, rapamycin treatment effectively ameliorated anemia phenotypes in the MLASA patient. Our findings provide novel insights into the crucial role of mitochondrial tRNA pseudouridylation in governing erythropoiesis and present potential therapeutic strategies for anemia patients facing challenges related to protein translation.

## Introduction

Pseudouridine is the most abundant RNA modification found in tRNA, rRNA, and mRNA.[1,2] It plays a vital role in RNA biology, affecting processes such as protein translation, pre-mRNA processing, and various cellular functions.[3,4] Pseudouridylation refers the process of converting uridine (U) into pseudouridine (Ψ) catalyzed by pseudouridine synthases (PUSs). Abnormal pseudouridylation has been associated with several human diseases,[5] for example PUS7-mediated pseudouridylation in stem cell commitment, leukemogenesis,[6,7] and glioblastoma.[8]

Erythropoiesis is a complex process with different stages, and any disturbances can result in anemia.[9] Sideroblastic anemia (SA) is a type of anemia characterized by ring sideroblasts. The pathogenic genes associated with congenital sideroblastic anemia (CSA) such as LARS2, ABCB7 and ALAS2,[10-12] are predominantly involved in pathways involving mitochondria, such as heme biosynthesis, iron-sulfur cluster biogenesis, mitochondrial translation and respiration, indicating a relationship of anemia and mitochondria. A rare form of SA, known as mitochondrial myopathy, lactic acidosis, and sideroblastic anemia (MLASA), involves multi-system defects and is associated with mutations in three genes: pseudouridine synthase 1 (*PUS1*),[13-24] mitochondrial tyrosine tRNA synthetase (*YARS2*), and *MT-ATP6* gene.[11] PUS1 is the first gene identified in connection with MLASA, but the roles of PUS1 in erythropoiesis remains unclear.

In this study, we investigated the effects of pseudouridylation in erythropoiesis with MLASA patient-derived induced pluripotent stem cell (iPSC) lines and a corresponding *Pus1* mutant mouse model. We identified that PUS1 deficiency leads to altered tRNA pseudouridylation, resulting in decreased protein synthesis and subsequent anemia. We further explored the potential use of an mTOR inhibitor to alleviate the anemia phenotype in MLASA patients.

## Methods

### Clinical samples

The patient and her parents signed informed consent to utilize their clinical data and blood samples in this study in accordance with the Declaration of Helsinki. patient sample usage has been approved by the Ethics Advisory Committee of the Institute of Hematology and Blood Diseases Hospital (NSFC2021073-EC-2). For the exploratory treatment in this case, we obtained written authorization from the patient and her parents to use the off-label drug sirolimus.

### Human iPSC culture

Human iPSCs and ESCs were maintained in Matrigel-coated in E8 medium or mTeSR1™ medium (STEMCELL) according to the manufacturer's manual as previously described.[25]

### Generation of mouse model

All experiments were conducted under the institutional guidelines of the Institutional Animal Care and Use Committee of State Key Laboratory of Experimental Hematology. For details see supplementary methods.

### Statistical analysis

All data statistics were processed using GraphPad Prism 8 and presented as Mean±SD. One-way ANOVA, two-way ANOVA and unpaired Student's t-test were used for variance analysis, *$P$<0.05; **$P$<0.01; ***$P$<0.001.

Research using patient samples has been approved by the Ethics Advisory Committee of the Institute of Hematology and Blood Diseases Hospital. All experiments were conducted under the institutional guidelines of the Institutional Animal Care and Use Committee of State Key Laboratory of Experimental Hematology.

## Results

### A novel *PUS1* p.P175fs mutation identified in a MLASA patient

A 16-year-old female patient was admitted to our hospital with self-reported exercise intolerance, long-term pallor, and undue fatigue in 2013. The patient has a history of anemia and was first diagnosed at 6 months' old in a local hospital (Supplemental Table 1). Complete blood count suggested macrocytic anemia (HGB 46 g/L; RBC $1.33\times10^{12}$/L; HCT, 16.1%; MCV, 121.1 fL). Blood tests also presented hyperlactacidemia (lactate 2.4 mmol/L, normal range 1.0–1.8 mmol/L). B-ultrasound revealed splenomegaly, while her hepatic functional test results were normal. The bone marrow (BM) aspiration revealed dysplastic erythropoiesis with 12% ring sideroblasts (Figure 1A). Based on the above findings, the patient was diagnosed with SA. Transfusion of RBCs only achieved a short-term relief. In the subsequent six years, the patient was prescribed with various medications including folic acid, vitamin B1 or vitamin B6. However, the hemoglobin level showed no improvement (Figure 1B and Supplemental Table 2).

We then performed targeted sequencing for 636 genes related to hematological and genetic diseases (Supplemental Table 3) with peripheral blood (PB) cells of the patient and her parents. Notably, a novel homozygous frameshift mutation resulting in a premature stop codon in the amino acid 183 (c.523delC, p.P175fs*8; NM 025215.6) of *PUS1* gene was identified in the patient, while the other recognized mutations were all heterozygous (Supplemental Table 4). This mutation in *PUS1* was verified by Sanger sequencing, and her parents carried the same heterozygous variant, indicating this mutation is inherited (Figure 1C). *PUS1* mutations have been reported to cause MLASA, and P175 was found to locate in the most mutated catalytic domain (Supplemental Figure 1A)[13-23]. The patient was then preliminarily diagnosed as MLASA, with a new *PUS1* P175fs mutation.

**The P175fs mutation in *PUS1* results in a reduction of its mRNA and a loss of the protein**

To ascertain that *PUS1* P175fs mutation causes MLASA in this patient and the underlying pathogenesis, we established a patient-derived-inducible pluripotent stem cell (iPSC) line (MLASA-iPSCs) by introducing Yamanaka factors into isolated BM mononuclear cells from patient by electroporation (Supplemental Figure 1B) since *in vitro* patient-derived iPSC model is suitable for disease pathogenesis analysis and drug screening. A cell line with repaired mutation (MLASA-Res-iPSCs) by CRISPR-Cas9 to introduce the missing cytosine at position 523 to the *PUS1* mutated gene via homologous repair (Supplemental Figure 1C) was also established. The mutation and correction of the *PUS1* gene were verified by Sanger sequencing in these iPSC lines (Supplemental Figure 1D), and the iPSCs derived from a healthy individual (Normal-iPSCs) were used as control.

The pluripotency of MLASA-iPSCs and MLASA-Res-iPSC was confirmed through mRNA and protein expression analysis of pluripotency markers by RT-qPCR, flow cytometry or immunofluorescence (IF) assay (Supplemental Figure 1E-G), and further confirmed by the generation of three germ layers in teratoma formation assays (Supplemental Figure 1H). All three iPSC lines tested were free of mycoplasma infection (Supplemental Figure 1I). A lower mRNA expression level and a complete absence of PUS1 protein (Supplemental Figure 1J-K) were observed in MLASA-iPSCs, which was restored in MLASA-Res-iPSCs.

**The deficiency of PUS1 leads to a blockade of erythropoiesis**

To examine whether the P175fs mutation affected erythropoiesis in patient-derived iPSC, we examined erythropoiesis of the iPSCs with four induction strategies. The first differentiation strategy involves a modified feeder- and xeno-free defined system with three stages (Figure 1D). In the tiling iPSC colony formation stage, MLASA-iPSCs formed dense colonies with normal morphology but in much smaller

size than those of Normal- or MLASA-Res-iPSCs (Figure 1Ei and 1F). Following 4 days of hematopoietic endothelial (HE, $CD34^+CD31^+$) cells induction in the 2nd stage, MLASA-iPSCs generated similar proportions of HE cells with Normal- or MLASA-Res-iPSCs (Figure 1Eii and 1G). After 7-day of erythropoiesis, HE cells derived from Normal-iPSCs could produce more than 10% erythroblasts ($CD71^+CD235a^+$), while few erythroblasts (about 0.04%) were observed in MLASA group, which was fully rescued in MLASA-Res-iPSCs (Figure 1Eiii and 1H). The red pellets of erythroblasts indicated the production of hemoglobin (Figure 1Eiv). We also evaluated the erythroblasts at multiple time points during the differentiation process, and the results showed that the cells derived from MLASA-iPSCs did not differentiate early or delayed, but rather arrested at proerythroblast/basophilic erythroblast stages (Supplemental Figure 2A-H).

Similar findings were observed using another two-stage erythroid differentiation strategy[26] (Figure 1I). After the first 6-day of hemogenic induction, the percentage of HE cells were similar between MLASA-iPSCs, Normal and MLASA-Res-iPSCs (Figure 1J and Supplemental Figure 2Fi). Following another 6-day of erythroid differentiation stage, while Normal-iPSCs and MLASA-Res-iPSCs produced more than 20% erythroblasts, MLASA-iPSCs only produce less than 10% erythroblasts (Figure 1K and Supplemental Figure 2Fii-H). Since the proportions of erythroblasts obtained by above two strategies were not high enough, we also optimized two normoxic differentiation methods, and obtained similar results (Supplemental Figure 3A-G, Supplemental Figure 4A-G). In conclusion, patient-derived MLASA-iPSCs have erythroid differentiation defects.

**The depletion of PUS1 impairs mitochondrial function**

Mitochondrial dysfunction has been reported in MLASA patients carrying various *PUS1* mutations.[20] Our patient complained of fatigue after exercise is an indication of mitochondrial dysfunction. A notably higher level of mitochondrial mass and a lower

ratio of MMP to mitochondrial mass (Figure 2A-B), which indicating compromised mitochondria function, were observed in MLASA-iPSCs that could be rectified in MLASA-Res-iPSCs. The mtDNA copy number of MLASA-iPSCs was comparable between Normal-iPSCs and MLASA-Res-iPSCs (Figure 2C). Only MLASA-iPSCs has significant reduced ATP production (Figure 2D), and elevated mitochondrial superoxide, cytoplasmic and total ROS levels (Figure 2E-G). More importantly, both the basal and maximum oxygen consumption rates (OCRs) were decreased in MLASA-iPSCs in comparison with Normal-iPSCs or MLASA-Res-iPSCs (Figure 2H-I). The activities of NADH dehydrogenase (complex I) and cytochrome c reductase (complex III) were attenuated while the activity of succinate-coenzyme Q reductase (complex II) was increased in MLASA-iPSCs (Figure 2J).

**Loss of pseudouridylation of PUS1 targeted mt-tRNAs affects the abundance of mitochondrial proteins**

Mitochondrial genome encodes 13 proteins, synthesized by mitochondrial ribosome and mt-tRNAs, are all components of the oxidative respiratory chain. As some mt-tRNAs have been reported to be the targets of PUS1[23] and pseudouridine can affect the stability of tRNAs,[27] we analyzed the mt-tRNA levels in MLASA- and MLASA-Res-iPSCs using mt-tRNA PCR array (Supplemental Table 5). Five of the 22 mt-tRNAs were differentially expressed, and all were down-regulated in the MLASA-iPSCs, namely mt-tRNA$^{Cys}$, mt-tRNA$^{Ser\ (UCN)}$, mt-tRNA$^{Ala}$, mt-tRNA$^{Tyr}$, and mt-tRNA$^{Gln}$ (Figure 3A). In view of the important role(s) of mt-tRNA for mitochondrial translation, we evaluated the overall mitochondrial translation of iPSCs by immunofluorescence. As expected, PUS1 deletion led to a decrease in mitochondrial protein synthesis (Supplemental Figure 5A-B). To further explore the potential mechanism, we identified mt-tRNA$^{Cys}$, mt-tRNA$^{Ser\ (UCN)}$, and mt-tRNA$^{Tyr}$ contain sites (position 28) that may be modified by PUS1 according to the reported PUS1 targeted sites and structural motifs (Figure 3B),[2,27] and confirmed that those sites were PUS1

targets by *N*-cyclohexyl-*N'*-(2-morpholinoethyl)carbodiimide (CMC) primer extension assay (Figure 3C).

We further investigated whether the above three PUS1-modified mt-tRNAs affect the translation of mitogenome-encoded proteins. The 13 proteins were ranked according to the sum of the usage frequency of codons complementary to these three mt-tRNAs (Figure 3D) and their protein levels were determined by the Western blot (Figure 3E-F). As expected, the protein level of first-ranked CYTB, the only component of complex III encoded by the mitochondrial genome (III:CYTB), was greatly decreased in MLASA-iPSCs (Figure 3E-F). The expression of the second ranked CIV:COX1, was also reduced, whereas the expression of CIV:COX2 and CV:ATP6, that ranked in the last one-thirds, showed an increase, suggesting that the overall mitochondrial translation was dysregulated due to PUS1 deficiency (Figure 3E-F). Since components of OXPHOS complex are coordinately synthesized by mitochondrial and cytosolic translation,[28] we examined the expression of several nuclear-encoded mitochondrial subunits and found that the protein levels of CIII:UQCRC1, CIII:UQCRC2 and CI:NDUFB8 were greatly decreased in MLASA-iPSCs, while CII:SHDA and CV:ATP5A remain unchanged (Figure 3G-H). In conjunction with the decreased expression of mitochondrial-encoded CIII:CYTB, these results explain the reduced activities of Complex III and Complex I. Interestingly, although the protein levels were reduced, the mRNA levels of both mito- and nuclear-encoded mitochondria genes examined did not decrease, suggesting an underlying post-transcriptional mechanism (Figure 3I). The combined findings suggest that PUS1 regulates mitochondrial function via altering the abundance of mt-tRNAs by pseudouridylation, which synchronizes the cytoplasmic and mitochondrial translation of the subunits of OXPHOS complexes, consequently regulating their activities.

**Rapamycin alleviates erythroid differentiation arrest caused by PUS1 deficiency**

Since PUS1 deficiency leads to the loss of pseudouridine in mtRNA, resulting in abnormal mitochondrial and cytoplasmic protein synthesis, we performed RNA sequencing (RNA-Seq), ribosome sequencing (Ribo-Seq) and proteomics analyses with iPSCs from MLASA- and MLASA-Res- groups (Supplemental Figure 6A-G), to gain a whole picture of protein synthesis. The translation efficiency (TE) of genes was obtained by combined analysis of Ribo-seq and RNA-seq using X-tail.[29] The results showed that the up-regulated differential genes of TE were enriched in the mTOR signaling and OXPHOS pathway, while the differential genes of proteomics were also enriched in the OXPHOS pathway (Supplemental Figure 6C, 6F and Supplemental Table 6-8). Based on the above results, we selected mTOR inhibitors and mitochondrial function-related reagents for drug screening.[30-32] Interestingly, while nicotinamide ribose (NR) treatment improved the mitochondrial function MLASA-iPSCs (Supplemental Figure 7A-D), the efficiency of erythropoiesis was not improved (Supplemental Figure 7E), so were coenzyme Q10 (CoQ10) and its analogue mitoquinone (MitoQ) in MLASA-iPSCs (Supplemental Figure 7F-I). Several other metabolic-related compounds[33] screened did not improve the erythroid differentiation of MLASA-iPSCs either (Supplemental Figure 7J-K, Supplemental Table 9).

Interestingly, we found that rapamycin, an inhibitor of mTOR pathway (Supplemental Figure 8A), improved the erythroid differentiation in MLASA-iPSCs (Figure 4A and Supplemental Figure 8B-G), while the proportion of erythroblasts in the Normal and MLASA-Res groups treated with rapamycin was significantly reduced (Figure 4A, Supplemental Figure 8F-G), indicating that the therapeutic effect of rapamycin for MLASA group is specific. Subsequent Western blot and flow cytometry analyses revealed a higher phosphorylation level of ribosomal protein S6 (S6) and eukaryotic translation initiation factor 4E (eIF4E)-binding proteins (4E-BP1) in

MLASA-iPSCs and MLASA-HEs (Figure 4B-D), suggesting an activation of mTOR complex I (mTORC1) signaling in MLASA-cells. More than half of 94 mTORC1-targeted mRNAs, containing 5′ terminal oligopyrimidine (TOP) or TOP-like motifs[34,35], have up-regulated translation efficiency, most of which are cytoplasmic ribosomal proteins (Figure 4E; Supplemental Table 8). Furthermore, puromycin incorporation assay showed that the global level of protein synthesis was higher in MLASA-iPSCs than MLASA-Res-iPSCs (Figure 4F). Consistent with elevated protein synthesis in iPSCs, we also observed a higher protein synthesis rate of HE cells derived from MLASA group than MLASA-Res group (Figure 4G). Further rapamycin treatment of MLASA HE cells resulted in a marked reduction in global translation (Figure 4H). Our data thus indicated that rapamycin improved erythroid differentiation arrest caused by PUS1-deletion probably via inhibiting global protein synthesis.

To investigate the link between hyperactivated mTOR signaling pathway and abnormalities of OXPHOS, we treated Normal-iPSCs with complex III inhibitors antimycin A (AA) and 4NQO, and found activation of mTOR signaling pathway (Figure 4I-N). However, rapamycin treatment of iPSCs did not improve the mitochondrial function (Supplemental Figure 9A-G). These data indicate that complex III inhibition activates mTOR signaling pathway in iPSCs.

**PUS1-deficient mice exhibited anemia**

The highly conserved amino-acid sequence between murine PUS1 (mPUS1) and human PUS1 (hPUS1) (Supplemental Figure 10A) prompted us to establish and study a corresponding mouse model *Pus1*$^{S172fs/S172fs}$ (S172fs), mimicking patient P175fs mutation (Supplemental Figure 10B-C). No off-target effects were observed due to the editing of mutant mice (Supplemental Figure 10D-E). Consistent with patient-specific iPSC, the S172fs mutation led to mRNA reduction and protein loss (Supplemental Figure 11A-B) in mice. Further, no protein was detected by overexpression of N-terminal Flag-tagged mPUS1 carrying S172fs in MEL cell line

(Supplemental Figure 11C). Using CMC primer extension assay, we observed a loss of pseudouridine in mt-tRNA$^{Ile}$, suggesting that other members of PUS family were unable to compensate for mPUS1 deficiency (Supplemental Figure 11D-E).

The 4-week-old S172fs mice showed significant reduced body and spleen weight when compared to wild-type (WT) mice, with no difference in spleen/body weight ratio (Supplemental Figure 11F-I). The complete blood count (CBC) analysis revealed that the S172fs mice exhibited significant lower levels of RBCs, HGB and HCT than those of WT mice, indicating the presence of anemia, regardless of gender (Figure 5A, Supplemental Figure 11J). Furthermore, the frequency and absolute count of proerythroblasts (proE, CD71$^{+}$Ter119$^{int}$, int, intermediate) and basophilic erythroblasts (CD71$^{high}$Ter119$^{+}$) in the BM of S172fs mice were significantly increased, while the frequency of late basophilic and chromatophilic erythroblasts (CD71$^{int}$Ter119$^{+}$) and orthochromatophilic erythroblasts (CD71$^{-}$Ter119$^{+}$) were significantly decreased, indicating a blockage of erythroid maturation in BM of S172fs mice (Figure 5B-D). Similarly, the spleen of the S172fs mice exhibited arrested erythroid development (Figure 5E-G). Similar to the erythrocytes derived from MLASA-iPSCs, no ring sideroblasts were observed in S172fs BM cells stained by Prussian blue (Supplemental Figure 11K). Further, both female and male mutant mice exhibited impaired erythropoiesis in the BM (Supplemental Figure 12A-B), indicating that the effect of S172fs on erythropoiesis is gender independent in mice.

Consistent with the previous established *PUS1* knockout mouse model,[36] the S172fs mutant mice did not display anemia at 7-8 weeks (Supplemental Figure 12C), yet exhibited impaired erythropoiesis in both BM and SP of S172fs mice (Supplemental Figure 12D-E). Therefore, the anemia phenotype observed in our mouse model is specific to the 4-week-old mice.

To investigate the underlying causes of abnormal erythroid differentiation in S172fs mice, the hematopoietic stem and progenitor cells (HSPCs) and erythroid precursor cells were examined. We found that the frequencies of lineage$^{-}$c-Kit$^{+}$Sca-1$^{+}$

(LSK) and short-term HSCs (ST-HSC) were slightly increased in S172fs mice at 4 weeks, independent of gender (Supplemental Figure 13A-K). Serial competitive transplantation experiments revealed impaired functionality of hematopoietic stem cells in terms of self-renewal and multi-lineage differentiation in S172fs mice (Figure 5H-I and Supplemental Figure 14A-E). Collectively, our findings establish that PUS1 plays an important role in regulating erythroid differentiation both *in vitro* and *in vivo*, and its deficiency impairs erythropoiesis.

**PUS1-deficient mice exhibited mitochondrial dysfunction**

We further investigated mitochondrial functions in HSPCs from mutant and WT mice, and found an upregulation in mitochondrial mass in HSCs, GMPs, and CMPs within the S172fs group (Figure 6A). Additionally, we observed an increase in MMP specifically in HSCs and MPPs in the S172fs group (Figure 6B). Cytoplasmic and mitochondrial ROS level were relatively stable in HSPCs (Supplemental Figure 15A-B). We observed a slightly increased mitochondrial biomass, reduced MMP, and elevated cytoplasmic ROS in BM Ter119$^+$ erythroid cells in 4-week-old S172fs mice (Figure 6C-E). No significant differences were observed in the mitochondrial ROS levels of BM Ter119$^+$ cells (Figure 6F), and the mitochondrial mass and ROS levels of SP erythroid cells (Supplemental Figure 15C-F) between two groups. The copy numbers of mtDNA in both BM and spleen cells were similar between two groups (Supplemental Figure 7G-H). Thus, it appears that the mitochondrial functions of HSPCs are more susceptible to the effects of PUS1 deletion than in erythroblasts. Similar to the results observed in iPSCs, the basal and maximum oxygen consumptions of erythrocytes (Ter119$^+$) from S172fs mice were lower than that of WT (Figure 6G-H). In addition, the activity of complex III was significantly decreased in hematopoietic cells of the mutant group, while that of complex II was increased (Figure 6I-J).

We found that mTOR signaling activation indicator 4E-BP1's phosphorylation levels were higher in both S172fs BM and spleen cells than controls (Figure 7A and Supplemental Figure 16A). Administration of rapamycin intraperitoneally to 3-week-old S172fs mice for 7 consecutive days partially recovered the PB values of RBC, HGB and HCT of S172fs mice than vehicle-treatment group (Figure 7B-E).

In addition, a delayed erythroid differentiation (Supplemental Figure 16B-C) and enhanced activation of the mTOR signaling pathway (Supplemental Figure 16D-G) were observed in WT $Lin^-$ cells when treated with complex III inhibitor AA in erythroid differentiation experiments[37], indicating that complex III inhibition triggers the activation of the mTOR signaling pathway and potentially abnormalities in erythroid differentiation. These findings collectively demonstrate that the loss of PUS1 leads to mitochondrial dysfunction, both *in vitro* and *in vivo*.

Furthermore, the effects of rapamycin in mutant HSC function were evaluated with competitive transplantation assay (Supplemental Figure 17A). Elevated phosphorylation of S6 in mutant BM cells were significantly reduced after rapamycin treatment (Supplemental Figure 17B). Rapamycin-treated mutant cells showed increased reconstitution of RBCs than mutant-vehicle cells (Supplemental Figure 17C-D), albeit still significantly lower than WT-vehicle groups (Supplemental Figure 17C-I). Thus, rapamycin partially improves the impaired erythropoietic reconstitution, while its impact on other hematopoietic lineages is not significant.

**Rapamycin effectively ameliorates abnormal erythroid differentiation in the MLASA patient**

Previous studies showed that hyper-activated mTORC1 caused macrocytic anemia while hypo-activated mTORC1 led to microcytic anemia.[38] Interestingly, our MLASA patient exhibited macrocytic anemia and hyper-activated mTORC1. Based on the encouraging results of rapamycin treatment in MLASA-iPSCs and S172fs mice, and its established clinical safety, we hypothesized that inhibiting mTOR signaling

pathway could alleviate anemia in MLASA patients. The MLASA patient was administered with sirolimus (rapamycin) at a dosage of 1 to 2.5 mg per day under strict supervision and medical guidance (Figure 7F-M). Remarkably, within one-month of treatment，the patient’s blood HGB content significantly increased to 94 g/L, a level that had never been reached before in the patient’s clinical history. The RBC count and HCT values also increased. The value of RDW-CV decreased with sirolimus treatment, indicating an improvement in the size uniformity of the patient's RBCs, and normal WBC count. The serum level of sirolimus in MLASA patient was 13.92 ng per milliliter, an effective and safe therapeutic concentration in the human body.[39] The patient continued sirolimus treatment for one year, and the benefits sustained. These data strongly suggest that suppression of aberrantly activated mTORC1 signaling can be beneficial for MLASA patients in terms of alleviating anemia.

## Discussion

The cellular and molecular processes connecting pseudouridylation to erythroid differentiation have not been clearly elucidated over nearly 30 years since the first report of MLASA with a *PUS1* genetic mutation.[18] Here, we utilized *in vitro* patient-specific iPSC and *in vivo* mouse models, demonstrated that PUS1 deficiency causes altered pseudouridine modification of specific mt-tRNAs, resulting in disordered mitochondrial biogenesis. This disruption leads to mitochondrial dysfunction and aberrant activation of the mTOR signaling pathway. Ultimately, these molecular events culminate in the blockage in erythroid differentiation and the development of anemia. Importantly, the administration of rapamycin, an mTOR inhibitor, effectively relieved anemia in disease models as well as in the MLASA patient. Through our work, we have defined the role of pseudouridylation in erythropoiesis and anemia, thus offering valuable insights for the treatment of anemia in CSA and potentially other relevant disorders.

Our study further clarified the role of pseudouridine in mt-tRNA. In humans, although the PUS1-catalyzed Ψ formation at multi-positions of mt-tRNA has been reported,[27] their effect on mt-tRNAs are not fully elucidated. We showed that the presence of PUS1-targeted pseudouridine at position 28 of mt-tRNA$^{Cys}$, mt-tRNA$^{Ser(UCN)}$ and mt-tRNA$^{Tyr}$, enhanced their stability, which were consistent with previous studies indicating that pseudouridine could increase the thermodynamic stability of tRNAs.[40] The absence of specifically modified tRNAs can lead to translation stalling and impaired protein synthesis,[41] was also observed in mt-tRNAs and mitochondrial-encoded proteins CYTB and COX1, leading to impaired mitochondria respiration in MLASA cells. These new findings provided a clearer sequential event linking pseudouridylation to OXPHOS and mitochondrial function.

In our study, both patient-derived iPSCs and S172fs mice exhibited multiple mitochondrial abnormalities and a blockage in erythroid differentiation. Rapamycin could effectively improve the erythroid differentiation but did not ameliorate

mitochondrial function in patient-derived iPSCs and S172fs mice, while complex III inhibitors could activate the mTOR signaling pathway in both iPSCs and mouse cells. It is well-recognized that dysregulated mTOR signaling plays a crucial role in erythropoiesis and hematopoietic stem cell (HSC) function.[38,42] Knight et al. demonstrated that mTORC1 is regulated by dietary iron, and that activation or inhibition of mTORC1 by overexpression or ablation of Raptor results in macrocytic or microcytic anemia.[38] The activation of the mTOR signaling pathway is known to be governed by multiple factors, including metabolic signals such as glucose, amino acids, growth factors, hormones, cytokines, cellular iron content, and oxidative stress.[43,44] Therefore, the mTOR activation observed with PUS1 deletion may not solely stem from the defect in the enzyme activity of complex III, and needs further exploration.

Additionally, our findings highlight the intricate relationship and the interplay between mitochondrial dysfunction and the development of anemia in CSA or in other non-CSA anemia, when comprehensive treatment approaches to target multiple aspects of mitochondrial function in treating anemia more effectively is needed. Indeed, we observed that long-term usage of mTOR inhibitor sirolimus effectively alleviated anemia symptoms and improved the blood profile of this specific MLASA patient, without noticeable side effects. This improvement could be attributed to a combination of factors, such as directly correcting hyper-activation of mTOR signaling to erythroid differentiation, or restoring aberrant ribosome biogenesis to a more sustainable level. Currently, treatment options for CSA patients, including blood transfusions, iron removal, or other therapeutic approaches, have limited efficacy or yielded inconsistent or ineffective results due to the heterogeneity of the diseases.[45,46] Interestingly, while our studies demonstrated that sirolimus, an mTOR inhibitor, improved erythropoiesis and corrected anemia in the patient, sirolimus was used to treat refractory/relapsed/intolerant acquired pure red cell aplasia and refractory autoimmune hemolytic anemia.[47,48] Our new treatment regimen may be suitable for

anemia patients with mitochondrial dysfunction and/or stress-induced mTOR over-activation. Further clinical trials are necessary to validate this hypothesis and to provide more substantial evidence for the use of sirolimus in the treatment of anemia associated with mitochondrial dysfunction.

## Acknowledgements

This work was supported by funds from National Key R&D Program of China (2022YFA1103300 to WPY and YJC, 2020YFE0203000 to YJC); the National Natural Science Foundation of China (82150710556 and 82170135 to WPY, 82170117 to YJC，82270145 to SJ); the Chinese Academy of Medical Sciences Innovation Fund for Medical Sciences, CIFMS (2021-I2M-1-040 to WPY, 2021-I2M-1-073 to SJ); Haihe Laboratory of Cell Ecosystem Innovation Fund (HH22KYZX0037 to WPY and YJC), and Natural Science Foundation of Tianjin City (21JCYBJC01170 to YJC).

## Authorship Contributions

JS, YJC and WPY conceived the project, supervised the research and revised the paper. BCW, DYS, SY, YL and YJC designed and performed most of the experiments, wrote and revised the paper. HYL, MTC, YFH, LLZ, CQ, TL and WW assisted with experiments and data analysis, YWM, LS, TC and LHS contributed to the research design and paper discussion.

## Disclosure of Conflicts of Interest

The authors declare that the research was conducted in the absence of any commercial or financial relationships that could be construed as a potential conflict of interest.

## References


1. Cohn WE. Pseudouridine, a carbon-carbon linked ribonucleoside in ribonucleic acids: isolation, structure, and chemical characteristics. *J Biol Chem*. 1960;235:1488-1498.

2. Carlile TM, Martinez NM, Schaening C, et al. mRNA structure determines modification by pseudouridine synthase 1. *Nat Chem Biol*. 2019;15(10):966-974.

3. Song J, Zhuang Y, Zhu C, et al. Differential roles of human PUS10 in miRNA processing and tRNA pseudouridylation. *Nat Chem Biol*. 2020;16(2):160-169.

4. Li X, Xiong X, Yi C. Epitranscriptome sequencing technologies: decoding RNA modifications. *Nat Methods*. 2016;14(1):23-31.

5. Cerneckis J, Cui Q, He C, Yi C, Shi Y. Decoding pseudouridine: an emerging target for therapeutic development. *Trends Pharmacol Sci*. 2022;43(6):522-535.

6. Guzzi N, Muthukumar S, Ciesla M, et al. Pseudouridine-modified tRNA fragments repress aberrant protein synthesis and predict leukaemic progression in myelodysplastic syndrome. *Nat Cell Biol*. 2022;24(3):299-306.

7. Guzzi N, Ciesla M, Ngoc PCT, et al. Pseudouridylation of tRNA-Derived Fragments Steers Translational Control in Stem Cells. *Cell*. 2018;173(5):1204-1216 e1226.

8. Cui Q, Yin K, Zhang X, et al. Targeting PUS7 suppresses tRNA pseudouridylation and glioblastoma tumorigenesis. *Nat Cancer*. 2021;2(9):932-949.

9. An X, Schulz VP, Li J, et al. Global transcriptome analyses of human and murine terminal erythroid differentiation. *Blood*. 2014;123(22):3466-3477.

10. Ducamp S, Fleming MD. The molecular genetics of sideroblastic anemia. *Blood*. 2019;133(1):59-69.

513 11. Burrage LC, Tang S, Wang J, et al. Mitochondrial myopathy, lactic acidosis, and
514 sideroblastic anemia (MLASA) plus associated with a novel de novo mutation (m.8969G>A)
515 in the mitochondrial encoded ATP6 gene. *Mol Genet Metab*. 2014;113(3):207-212.
516 12. Zhang Y, Zhang J, An W, et al. Intron 1 GATA site enhances ALAS2 expression
517 indispensably during erythroid differentiation. *Nucleic Acids Res*. 2017;45(2):657-671.
518 13. Tesarova M, Vondrackova A, Stufkova H, et al. Sideroblastic anemia associated with
519 multisystem mitochondrial disorders. *Pediatr Blood Cancer*. 2019;66(4):e27591.
520 14. Bykhovskaya Y, Casas K, Mengesha E, Inbal A, Fischel-Ghodsian N. Missense
521 mutation in pseudouridine synthase 1 (PUS1) causes mitochondrial myopathy and
522 sideroblastic anemia (MLASA). *Am J Hum Genet*. 2004;74(6):1303-1308.
523 15. Fernandez-Vizarra E, Berardinelli A, Valente L, Tiranti V, Zeviani M. Nonsense
524 mutation in pseudouridylate synthase 1 (PUS1) in two brothers affected by myopathy,
525 lactic acidosis and sideroblastic anaemia (MLASA). *BMJ Case Rep*. 2009;2009.
526 16. Finsterer J. Comment on: Sideroblastic anemia associated with multisystem
527 mitochondrial disorders: The phenotypic spectrum of PUS1 and COX10 variants and
528 mtDNA deletions needs to be prospectively assessed. *Pediatr Blood Cancer*.
529 2019;66(11):e27945.
530 17. Zeharia A, Fischel-Ghodsian N, Casas K, et al. Mitochondrial myopathy, sideroblastic
531 anemia, and lactic acidosis: an autosomal recessive syndrome in Persian Jews caused by a
532 mutation in the PUS1 gene. *J Child Neurol*. 2005;20(5):449-452.
533 18. Oncul U, Unal-Ince E, Kuloglu Z, Teber-Tiras S, Kaygusuz G, Eminoglu FT. A Novel

PUS1 Mutation in 2 Siblings with MLASA Syndrome: A Review of the Literature. *J Pediatr Hematol Oncol*. 2021;43(4):e592-e595.

19. Fernandez-Vizarra E, Berardinelli A, Valente L, Tiranti V, Zeviani M. Nonsense mutation in pseudouridylate synthase 1 (PUS1) in two brothers affected by myopathy, lactic acidosis and sideroblastic anaemia (MLASA). *J Med Genet*. 2007;44(3):173-180.

20. Metodiev MD, Assouline Z, Landrieu P, et al. Unusual clinical expression and long survival of a pseudouridylate synthase (PUS1) mutation into adulthood. *Eur J Hum Genet*. 2015;23(6):880-882.

21. Cao M, Dona M, Valentino ML, et al. Clinical and molecular study in a long-surviving patient with MLASA syndrome due to novel PUS1 mutations. *Neurogenetics*. 2016;17(1):65-70.

22. Kasapkara CS, Tumer L, Zanetti N, Ezgu F, Lamantea E, Zeviani M. A Myopathy, Lactic Acidosis, Sideroblastic Anemia (MLASA) Case Due to a Novel PUS1 Mutation. *Turk J Haematol*. 2017;34(4):376-377.

23. Patton JR, Bykhovskaya Y, Mengesha E, Bertolotto C, Fischel-Ghodsian N. Mitochondrial myopathy and sideroblastic anemia (MLASA): missense mutation in the pseudouridine synthase 1 (PUS1) gene is associated with the loss of tRNA pseudouridylation. *J Biol Chem*. 2005;280(20):19823-19828.

24. Shi D, Wang B, Li H, et al. Pseudouridine synthase 1 regulates erythropoiesis via transfer RNAs pseudouridylation and cytoplasmic translation. *iScience*. 2024;27(3):109265.

555 25. Xu C, He J, Wang H, et al. Single-cell transcriptomic analysis identifies an
556 immune-prone population in erythroid precursors during human ontogenesis. *Nat Immunol*.
557 2022;23(7):1109-1120.
558 26. Zhu H, Kaufman DS. An Improved Method to Produce Clinical-Scale Natural Killer
559 Cells from Human Pluripotent Stem Cells. *Methods Mol Biol*. 2019;2048:107-119.
560 27. Borchardt EK, Martinez NM, Gilbert WV. Regulation and Function of RNA
561 Pseudouridylation in Human Cells. *Annu Rev Genet*. 2020;54:309-336.
562 28. Couvillion MT, Soto IC, Shipkovenska G, Churchman LS. Synchronized mitochondrial
563 and cytosolic translation programs. *Nature*. 2016;533(7604):499-503.
564 29. Xiao Z, Zou Q, Liu Y, Yang X. Genome-wide assessment of differential translations
565 with ribosome profiling data. *Nat Commun*. 2016;7:11194.
566 30. Lichtenstein DA, Crispin AW, Sendamarai AK, et al. A recurring mutation in the
567 respiratory complex 1 protein NDUFB11 is responsible for a novel form of X-linked
568 sideroblastic anemia. *Blood*. 2016;128(15):1913-1917.
569 31. Zhang H, Ryu D, Wu Y, et al. $NAD^+$ repletion improves mitochondrial and stem cell
570 function and enhances life span in mice. *Science*. 2016;352(6292):1436-1443.
571 32. Li C, Wu B, Li Y, et al. Amino acid catabolism regulates hematopoietic stem cell
572 proteostasis via a GCN2-eIF2alpha axis. *Cell Stem Cell*. 2022;29(7):1119-1134 e1117.
573 33. Rossmann MP, Hoi K, Chan V, et al. Cell-specific transcriptional control of
574 mitochondrial metabolism by TIF1$\gamma$ drives erythropoiesis. *Science*.
575 2021;372(6543):716-721.

576 34. Thoreen CC, Chantranupong L, Keys HR, Wang T, Gray NS, Sabatini DM. A unifying
577 model for mTORC1-mediated regulation of mRNA translation. *Nature*.
578 2012;485(7396):109-113.
579 35. Morita M, Gravel SP, Chénard V, et al. mTORC1 controls mitochondrial activity and
580 biogenesis through 4E-BP-dependent translational regulation. *Cell Metab*.
581 2013;18(5):698-711.
582 36. Mangum JE, Hardee JP, Fix DK, et al. Pseudouridine synthase 1 deficient mice, a
583 model for Mitochondrial Myopathy with Sideroblastic Anemia, exhibit muscle morphology
584 and physiology alterations. *Sci Rep*. 2016;6:26202.
585 37. Schneider RK, Schenone M, Ferreira MV, et al. Rps14 haploinsufficiency causes a
586 block in erythroid differentiation mediated by S100A8 and S100A9. *Nat Med*.
587 2016;22(3):288-297.
588 38. Knight ZA, Schmidt SF, Birsoy K, Tan K, Friedman JM. A critical role for mTORC1 in
589 erythropoiesis and anemia. *Elife*. 2014;3:e01913.
590 39. Shah PR, Kute VB, Patel HV, Trivedi HL. Therapeutic drug monitoring of sirolimus.
591 *Clinical Queries: Nephrology*. 2015;4(3-4):44-49.
592 40. Vissers C, Sinha A, Ming GL, Song H. The epitranscriptome in stem cell biology and
593 neural development. *Neurobiol Dis*. 2020;146:105139.
594 41. Suzuki T. The expanding world of tRNA modifications and their disease relevance. *Nat*
595 *Rev Mol Cell Biol*. 2021;22(6):375-392.
596 42. Liu X, Zhang Y, Ni M, et al. Regulation of mitochondrial biogenesis in erythropoiesis by

597 mTORC1-mediated protein translation. *Nat Cell Biol*. 2017;19(6):626-638.

598 43. Payne EM, Virgilio M, Narla A, et al. L-Leucine improves the anemia and
599 developmental defects associated with Diamond-Blackfan anemia and del(5q) MDS by
600 activating the mTOR pathway. *Blood*. 2012;120(11):2214-2224.

601 44. Gonzalez-Menendez P, Romano M, Yan H, et al. An IDH1-vitamin C crosstalk drives
602 human erythroid development by inhibiting pro-oxidant mitochondrial metabolism. *Cell*
603 *Rep*. 2021;34(5):108723.

604 45. Bachmeyer C, Ferroir JP, Eymard B, Maïer-Redelsperger M, Lebre AS, Girot R.
605 Coenzyme Q is effective on anemia in a patient with sideroblastic anemia and
606 mitochondrial myopathy. *Blood*. 2010;116(18):3681-3682.

607 46. Abu-Zeinah G, DeSancho MT. Understanding Sideroblastic Anemia: An Overview of
608 Genetics, Epidemiology, Pathophysiology and Current Therapeutic Options. *J Blood Med*.
609 2020;11:305-318.

610 47. Huang Y, Chen M, Yang C, Ruan J, Wang S, Han B. Sirolimus is effective for
611 refractory/relapsed/intolerant acquired pure red cell aplasia: results of a prospective
612 single-institutional trial. *Leukemia*. 2022;36(5):1351-1360.

613 48. Park JA, Lee HH, Kwon HS, Baik CR, Song SA, Lee JN. Sirolimus for Refractory
614 Autoimmune Hemolytic Anemia after Allogeneic Hematopoietic Stem Cell Transplantation:
615 A Case Report and Literature Review of the Treatment of Post-Transplant Autoimmune
616 Hemolytic Anemia. *Transfus Med Rev*. 2016;30(1):6-14.

617
618

## Figure legends

**Figure 1. *PUS1* p.P175fs mutation leads to abnormal erythroid differentiation.**

(A) Representative image of bone marrow iron stain of the patient with MLASA. Black arrows indicate ring sideroblasts. (B) Blood routine data of the patient from 2013 to 2019. Red dotted lines define the normal ranges. WBC, white blood cell; RBC, red blood cells; PLT, platelets; HGB, Hemoglobin; HCT, hematocrit; RDW-CV, Red blood cell volume distribution width-coefficient of variation; MCHC, mean corpuscular hemoglobin concentration; MCV, mean corpuscular volume. (C) Pedigree tree of the patient's family (left panel) and chromatograms of Sanger sequencing results (right panels). Patient has a homozygous *PUS1* mutation (c.523delC) is indicated by blackened symbols. Her parents carrying the same but heterozygous mutation are also indicated. The mutant proline at position 175 is marked with red, and the red arrow points to the location of the missing cytosine at position 523. (D) The schematic diagram of 3-stage erythroid differentiation from iPSCs. Green line: stage of tiling iPSC colony formation, orange line: stage of hemogenic induction, blue line: stage of erythroid differentiation. (E) Analysis of 3-stage erythroid differentiation efficiency at different stages. Representative images of iPSC colonies (i). Flow cytometry analysis of hemogenic endothelium cells (HEs) (ii) and erythroblasts (iii). Cell pellets of $CD71^{+}CD235^{+}$ cells and $CD71^{-}CD235^{-}$ cells produced by HEs *in vitro* for 7 days (iv). (F-H) Quantification of the sizes of iPSC colonies (F, Normal, n = 5; MLASA, n = 5; MLASA-Res, n = 6), the percentages of hemogenic endothelium cells (G,

CD34$^{+}$CD31$^{+}$, n = 3) and erythroblasts (H, CD71$^{+}$CD235a$^{+}$, n = 3). (I) The schematic diagram of iPSCs Normoxia Strategy I. Purple line: stage of hemogenic induction, brown line: stage of erythroid differentiation. (J-K) Quantification of the flow cytometry analysis of hemogenic endothelium cells (J, Normal, n = 4; MLASA, n = 5; MLASA-Res, n = 6), and erythroblasts (K, Normal, n = 2; MLASA, n = 3; MLASA-Res, n = 3) derived from iPSCs under normoxia induction strategy I. Values in all panels denote mean ± SD, *$P$ < 0.05, **$P$ < 0.01; one-way ANOVA.

**Figure 2. Loss of PUS1 impairs mitochondrial function in iPSCs.**

(A-B) Mitochondrial biomass (A) and the ratio of biomass to mitochondrial membrane potential (MMP, B) were evaluated in three iPSC lines by flow cytometry. The representative histogram (left) and Geometric mean fluorescent intensity (gMFI, right) are shown. Normal, n = 3; MLASA, n = 2; MLASA-Res, n = 3. (C) Quantitative analysis of mtDNA copy number via RT-qPCR in iPSCs. MT-LEU, mitochondria-tRNA$^{Leu}$; B2M, beta-2-microglobulin. n = 4. (D) Cellular ATP levels in iPSCs detected by CellTiter-Glo® 2.0 Reagent. n = 3. (E-G) Mitochondrial (E), total (F) and cytoplasmic (G) ROS levels of iPSCs were evaluated by MitoSOX, H2DCFDA and CellROX, respectively. The representative histogram (left) and gMFI (right) are shown. n = 3. (H-I) Measurement of cellular oxygen consumption in iPSCs. Oxygen consumption rates (OCRs) were monitored by injecting 1 μM oligomycin (Oligo), 0.5 μM FCCP, and 1μM rotenone/antimycin A (Rot/AA) in sequential order using the

Seahorse XFe24 Extracellular Flux Analyzer (H). The average basal and maximum respirations were normalized with Normal-iPSCs (I). n = 3. (J) Activity analyses of mitochondrial respiratory chain complexes. Complex I, II, III, IV, and V activities were measured according to the manuals of relevant kits. n = 3. Values in all panels denote mean ± SD, **P* < 0.05, ***P* < 0.01, ****P* < 0.001; one-way ANOVA.

**Figure 3. PUS1 regulates mitochondrial translation through downregulation of specific mitochondrial tRNAs.**

(A) Heat map of the amount of mitochondrial tRNAs (mt-tRNAs) differentially expressed in MLASA-iPSCs and MLASA-Res-iPSCs. *P* < 0.05 and fold change (FC) >1.2; n = 3. (B) Simplified secondary structures of five down-regulated mt-tRNAs in MLASA-iPSCs. Potential pseudouridine sites that may be modified by PUS1 are marked in red. The 5' and 3' ends of the tRNAs are labeled. The yellow arrows indicate the targeted regions of the designed primers for the CMCT primer extension assay. (C) Primers specific for mt-tRNA$^{Cys}$ (left), mt-tRNA$^{Ser(UCN)}$ (middle) or mt-tRNA$^{Tyr}$ (right) were used in primer extension reactions to determine the location of Ψ in MLASA and MLASA-Res iPSCs as described in Methods. The reverse transcription stops, corresponding to residue Ψ28, are labeled with red triangles. Full length indicated, the fragment from the beginning of the primer to the 5' end of the tRNA. Primer, the unbound primers. (D) Ranking according to the sum of usage frequency of codons complementary to mt-tRNA$^{Cys}$, mt-tRNA$^{Ser(UCN)}$ and mt-tRNA$^{Tyr}$ in each

mitochondrial-encoded protein. (E-F) Western blot analyses (E) and densitometry (F) of the mitochondrial-encoded proteins examined in iPSCs. Protein levels are normalized to β-actin or β-tubulin. n = 2. (G-H) Western blot analyses (G) and densitometry (H) of the nuclear-encoded oxidative respiratory chain proteins examined in iPSCs. Protein levels are normalized to β-actin or β -tubulin. n = 2. (I) RT-qPCR analyses for mRNA expression levels of some selected mitochondrial-encoded and nuclear-encoded oxidative respiratory chain genes in iPSCs. Expression levels are normalized to 18S. n = 3. Values in all panels denote mean ± SD, **P* < 0.05, ***P* < 0.01, ****P* < 0.001; unpaired Student's t-test.

**Figure 4. Rapamycin not NR alleviates the erythroid differentiation arrest caused by PUS1 deletion by inhibiting global protein synthesis.**

(A) Frequencies of the iPSC-derived erythroblasts after 7 days treatment with rapamycin under hypoxia conditions. Rapa, rapamycin. n = 3. (B) Phosphorylation levels of S6 (left) and 4E-BP1 (right) were examined by Western blot in iPSCs. Normalized to β-actin. (C-D) Phosphorylation levels of 4E-BP1 were measured by flow cytometry in iPSCs (C) and iPSC-derived HE cells (D). n = 3. (E) Pie chart representing the difference in translation efficiency of 94 TOP or TOP-like mRNAs between two iPSC lines. UP (purple) represents genes with increased TE in MLASA-iPSCs, while DOWN (azure) shows the decreased. NA (green) means the undetected genes, and NS (blue) no significant difference. (F) Global protein

synthesis was examined by puromycin incorporation in iPSCs. Western blot (left) and densitometry analyses (right) of the relative rate of protein synthesis are shown. Protein levels are normalized to β-tubulin. n = 3. (G) Protein synthesis rates monitored by OP-puro incorporation in HEs derived from iPSCs. The representative histogram (left) and MFI (right) of OP-puro are shown. n = 4. (H) Protein synthesis rates monitored by OP-puro incorporation in HE cells treated with rapamycin for 48 h during erythroid differentiation from HEs. The representative histogram (left) and MFI (right) of OP-puro are shown. n = 3. (I-J) Activity of Complex III in normal iPSCs with or without antimycin A (0.4 nM and 1.6 nM, n=3) (I) and 4NQO (100 nM, n=3) (J) treatment. (K-L) Phosphorylation levels of S6 (K) and 4E-BP1 (L) were examined by flow cytometry in normal iPSCs with or without antimycin A (0.4 nM and 1.6 nM). Representative graph (left) and frequency statistics (right) are shown. n = 4. (M-N) Phosphorylation levels of S6 (M) and 4E-BP1 (N) were examined by flow cytometry in normal iPSCs with or without 4NQO (100 nM). Representative graph (left) and gMFI (right) are shown. The gMFI was obtained using FlowJo 10.4 and the gMFI values of S6 and 4E-BP1 were normalized for each IgG background. n = 3. Values in all panels denote mean ± SD, **P* < 0.05, ***P* < 0.01, ****P* < 0.001; unpaired Student's t-test (C, D, F, G, J, M and N), one-way ANOVA (H, I, K and L) or two-way ANOVA (A).

**Figure 5. PUS1 deficiency impairs erythroid development in mice.**

(A) Complete blood count analysis of Wild-Type (WT) and *Pus1*$^{S172fs/S172fs}$ mice (S172fs) aged four weeks with different gender. Green dotted lines define the normal

ranges. Female mice at 4 weeks: WT, n = 7; S172fs, n = 11. Male mice: WT, n = 8; S172fs, n = 5. (B-D) Flow cytometry analysis of erythroblasts in bone marrow (BM) of mice aged four weeks. The gating strategy of erythroblasts by flow cytometry. R I to R IV represent proerythroblasts (Region I, $CD71^{high}Ter119^{int}$), basophilic erythroblasts (Region II, $CD71^{high}Ter119^{+}$), late basophilic and chromatophilic erythroblasts (Region, III, $CD71^{int}Ter119^{+}$), orthochromatophilic erythroblasts (Region IV, $CD71^{-}Ter119^{+}$), respectively. Representative graph (B), frequency statistics (C) and absolute numbers (D) of different stages are shown. WT, n = 11, 7 female mice and 4 male mice at 4 weeks; S172fs, n = 9, 7 female mice and 2 male mice at 4 weeks. (E-G) Flow cytometry analysis of erythroblasts in spleen (SP) cells of mice aged four weeks. Representative graph (E), frequency statistics (F) and absolute numbers (G) of different stages are shown. WT, n = 11, 7 female mice and 4 male mice at 4 weeks; S172fs, n = 9, 7 female mice and 2 male mice at 4 weeks. (H) Schematic diagram of serial competitive transplant assay. (I) Frequency of donor cells of mature erythrocytes in serial competitive transplant assay. Primary competitive transplantation n=7, 4 female mice and 3 male mice; secondary competitive transplantation n=6, 3 female mice and 3 male mice. Values in all panels denote mean ± SD $*P < 0.05$, $**P < 0.01$, $***P < 0.001$; unpaired Student's t-test (A), paired Student's t-test (I) or two-way ANOVA (C, D, F and G).

**Figure 6. PUS1 deficient mice exhibit mitochondrial dysfunction.**

(A-B) Mitochondrial biomass (A) and MMP (B) of $Lin^-$ / $LKS^-$ / $LSK^+$ / LT-HSC / ST-HSC / MPP / MEP / CMP / GMP cells were evaluated by flow cytometry. Female mice at 4 weeks, WT, n = 5; S172fs, n = 4. (C-D) Mitochondrial biomass (C) and MMP (D) of BM $Ter119^+$ cells were evaluated by flow cytometry. The representative histogram (left) and gMFI (right) are shown. Male mice at 4 weeks. WT, n = 6; S172fs, n = 3. (E-F) Cytoplasmic (E) and mitochondrial (F) ROS levels of BM $Ter119^+$ cells evaluated by CellROX and MitoSOX, respectively. The representative histogram (left) and gMFI (right) are shown. Male mice at 4 weeks. WT, n = 6; S172fs, n = 3. (G-H) Measurement of cellular oxygen consumption in BM $Ter119^+$ cells of mice. OCRs were monitored by injecting 1 μM Oligo, 2 μM FCCP, and 1μM Rot/AA in order using the Seahorse XFe24 Extracellular Flux Analyzer (G). The average basal and maximum oxygen consumptions were normalized to WT mice (H). n =6, male mice at 7-8 weeks. (I) Activities of mitochondrial respiratory chain complexes in WT and mutant mice. Complex I , II, III and IV (WT, n = 9-10; S172fs, n = 6, male mice at 7-8 weeks; Complex I , II and IV: BM cells; Complex III: SP cells) activities were measured according to the manuals of relevant kits. (J) Cellular ATP levels of BM cells between WT and S172fs groups were detected by CellTiter-Glo® 2.0 Reagent. WT, n = 10; S172fs, n = 6, male mice at 7-8 weeks. Values in all panels denote mean ± SD, $*P < 0.05$, $**P < 0.01$, $***P < 0.001$; unpaired Student's t-test (C-J) or two-way ANOVA (A and B).

**Figure 7. Rapamycin effectively ameliorates abnormal erythroid differentiation PUS1 deficient mice and MLASA patient.**

(A) Phosphorylation levels of 4E-BP1 were examined by Western blot in BM cells of mice. Protein levels are normalized to β-actin. (B-E) Complete blood count analysis of WT and *Pus1*-mutant mice with or without 4 mg/kg/day rapamycin treatment. RBC (B), HGB (C), HCT (D) and PLT (E) are shown. WT, n = 3; S172fs, n = 3, female mice at 4 weeks. Rapa, rapamycin. (F-I) Blood routine of RBC (F), HGB (G), HCT (H), MCV (I), RDW-CV (J), PLT (K), MCHC (L) and WBC (M) of the patient pre- and post-treatment with Sirolimus. Grey and lavender arrows indicate the time period of patients before and after sirolimus treatment, respectively. Values in all panels denote mean ± SD, **P* < 0.05, ***P* < 0.01; two-way ANOVA.

Figure 1

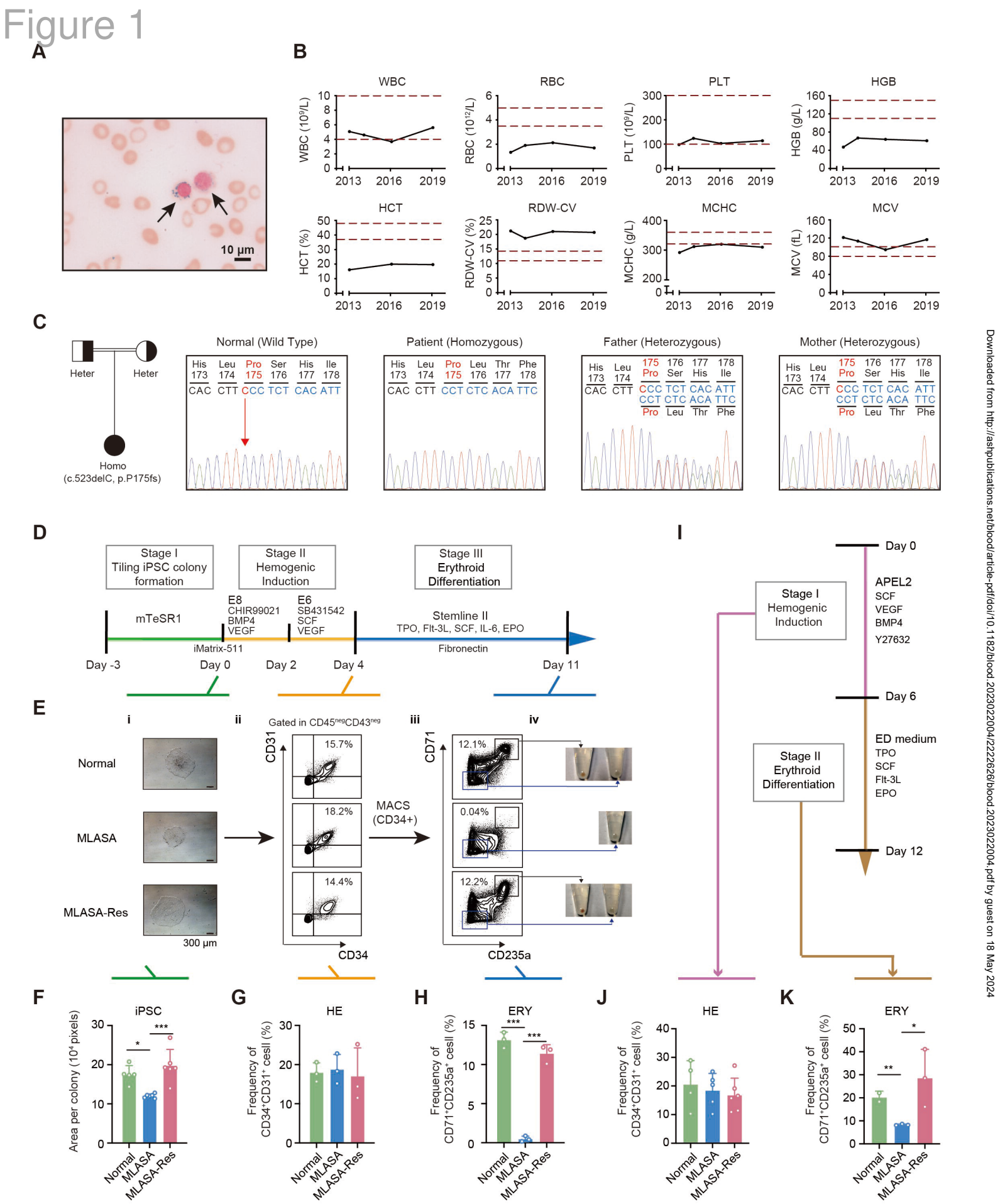

Figure 2

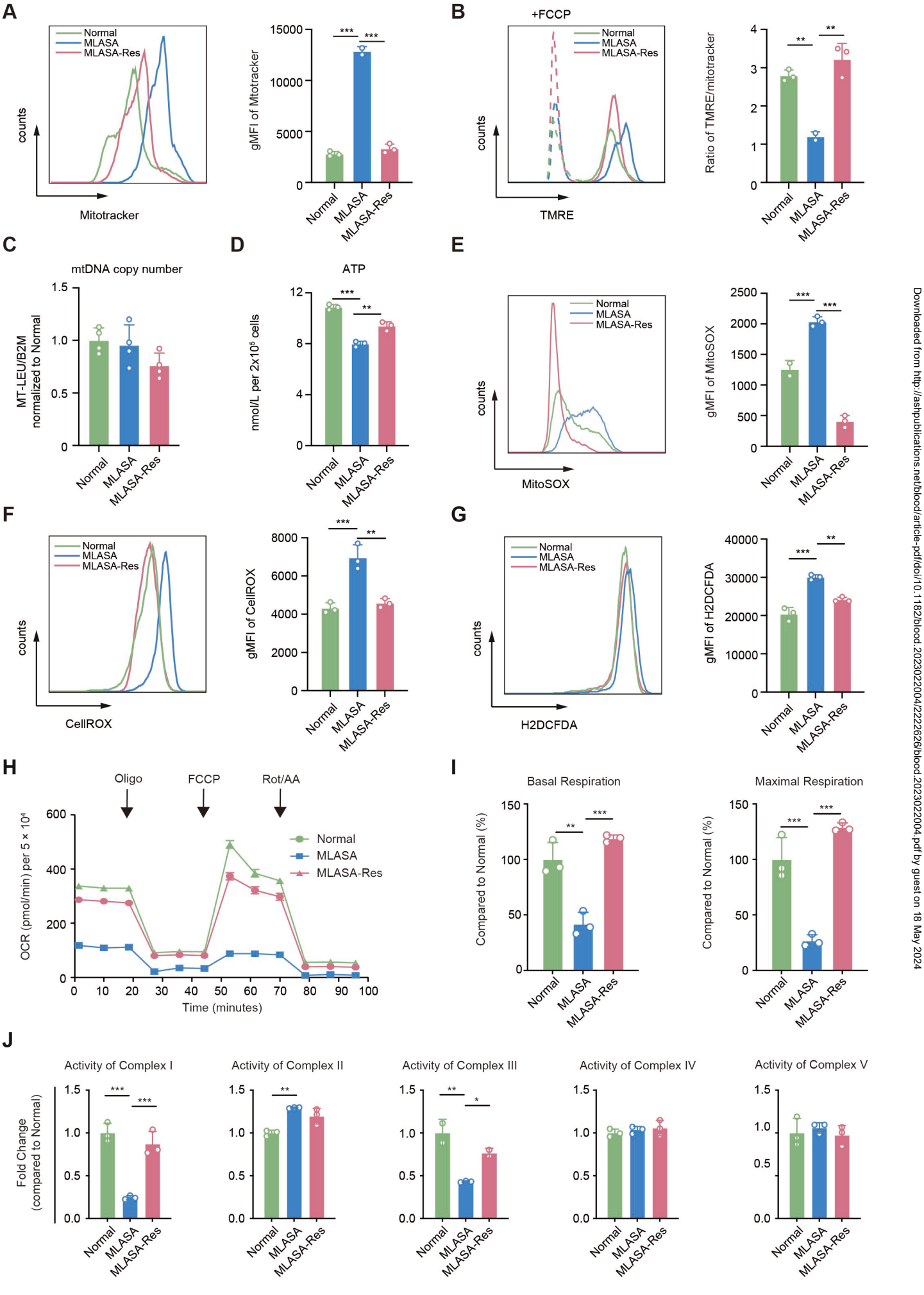

Figure 3

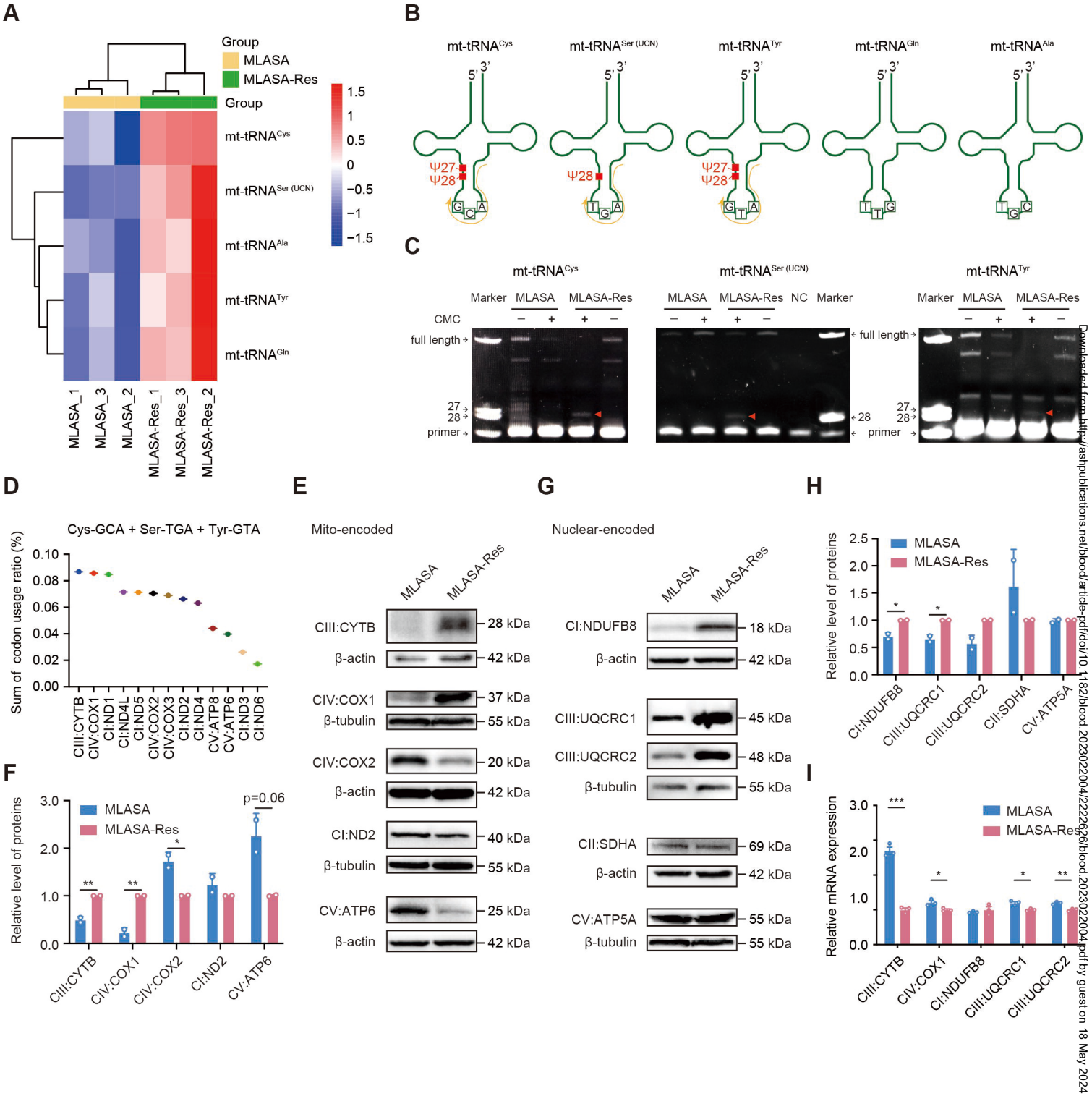

Figure 4

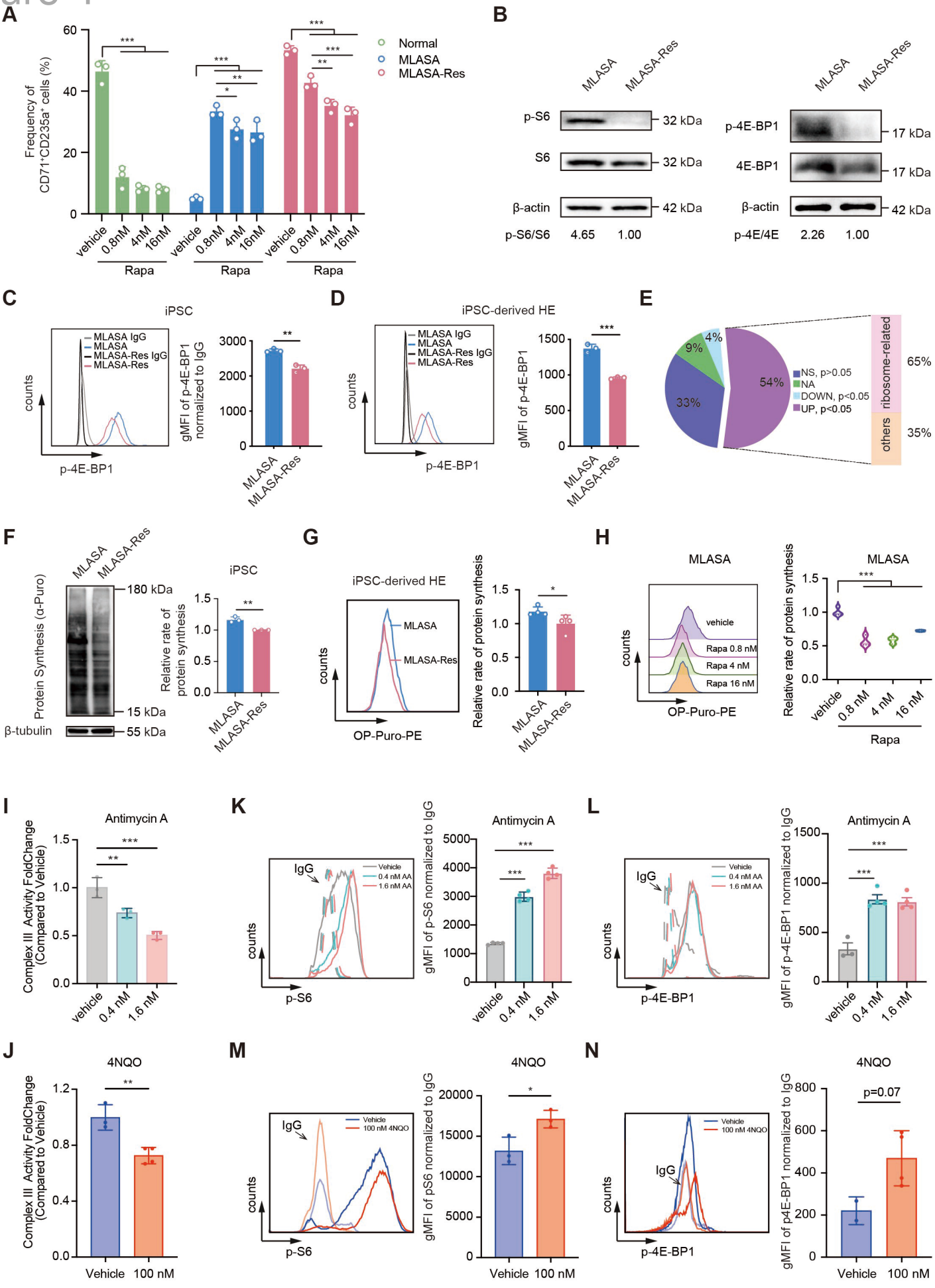

Figure 5

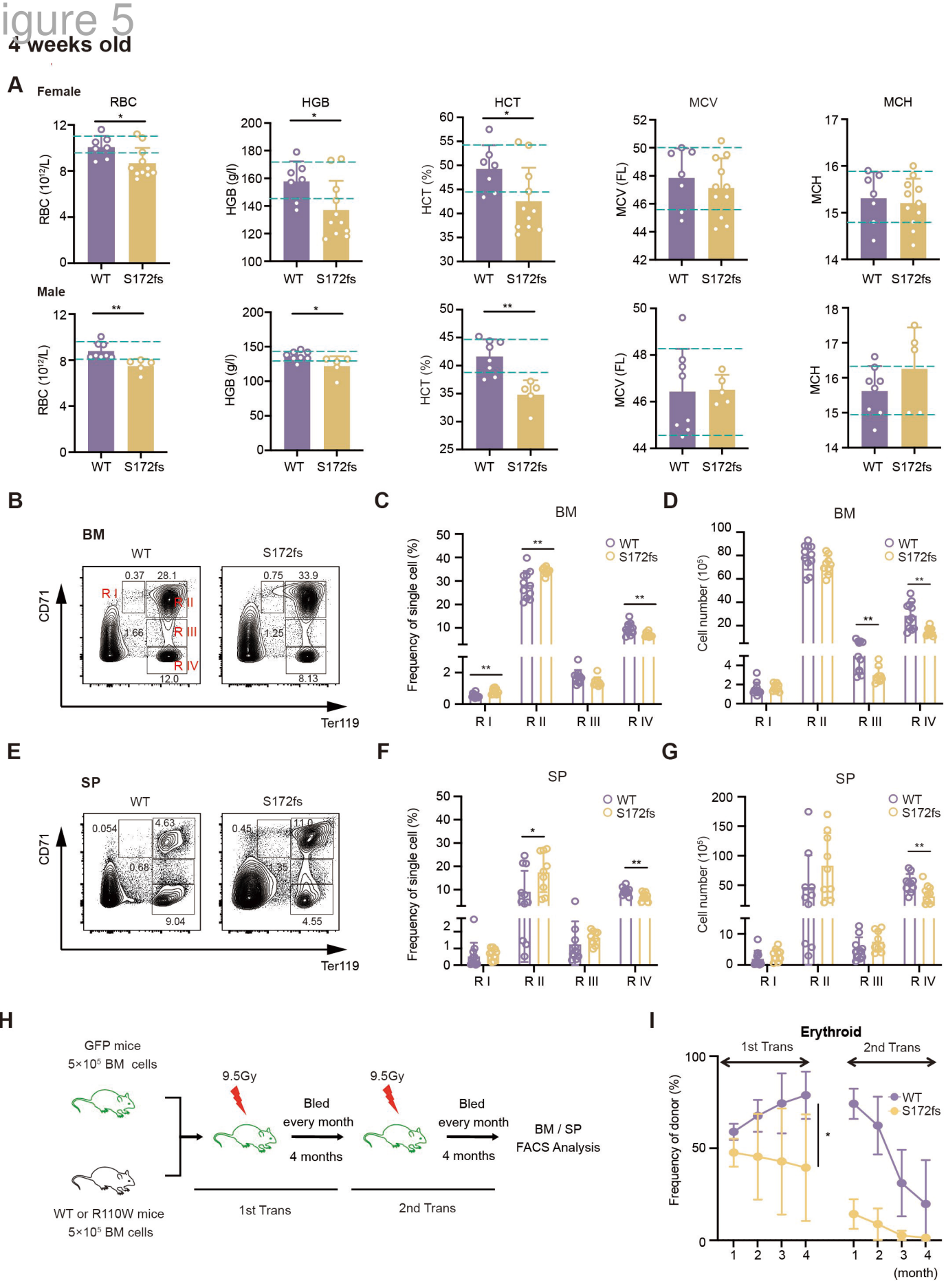

Figure 6

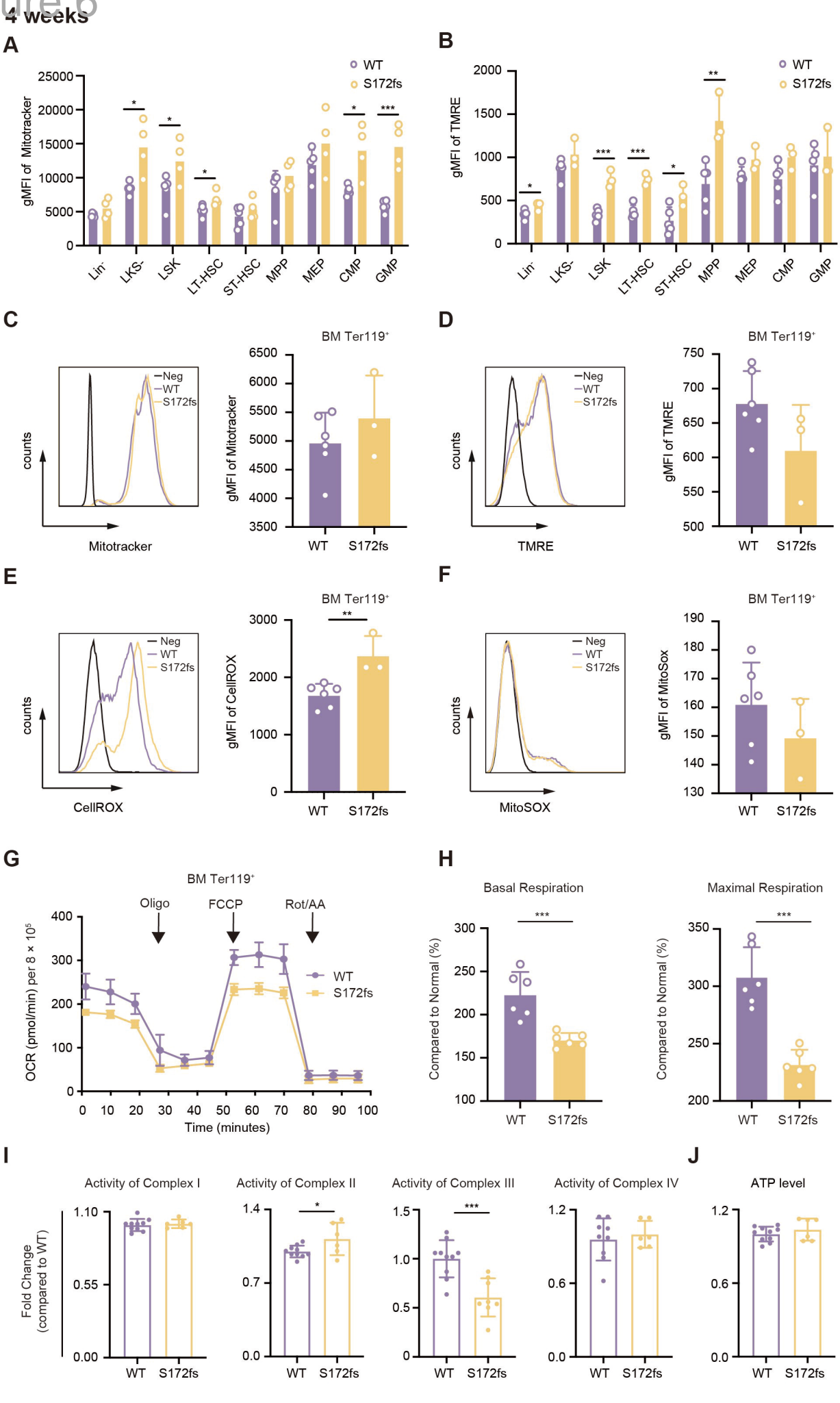

Figure 7

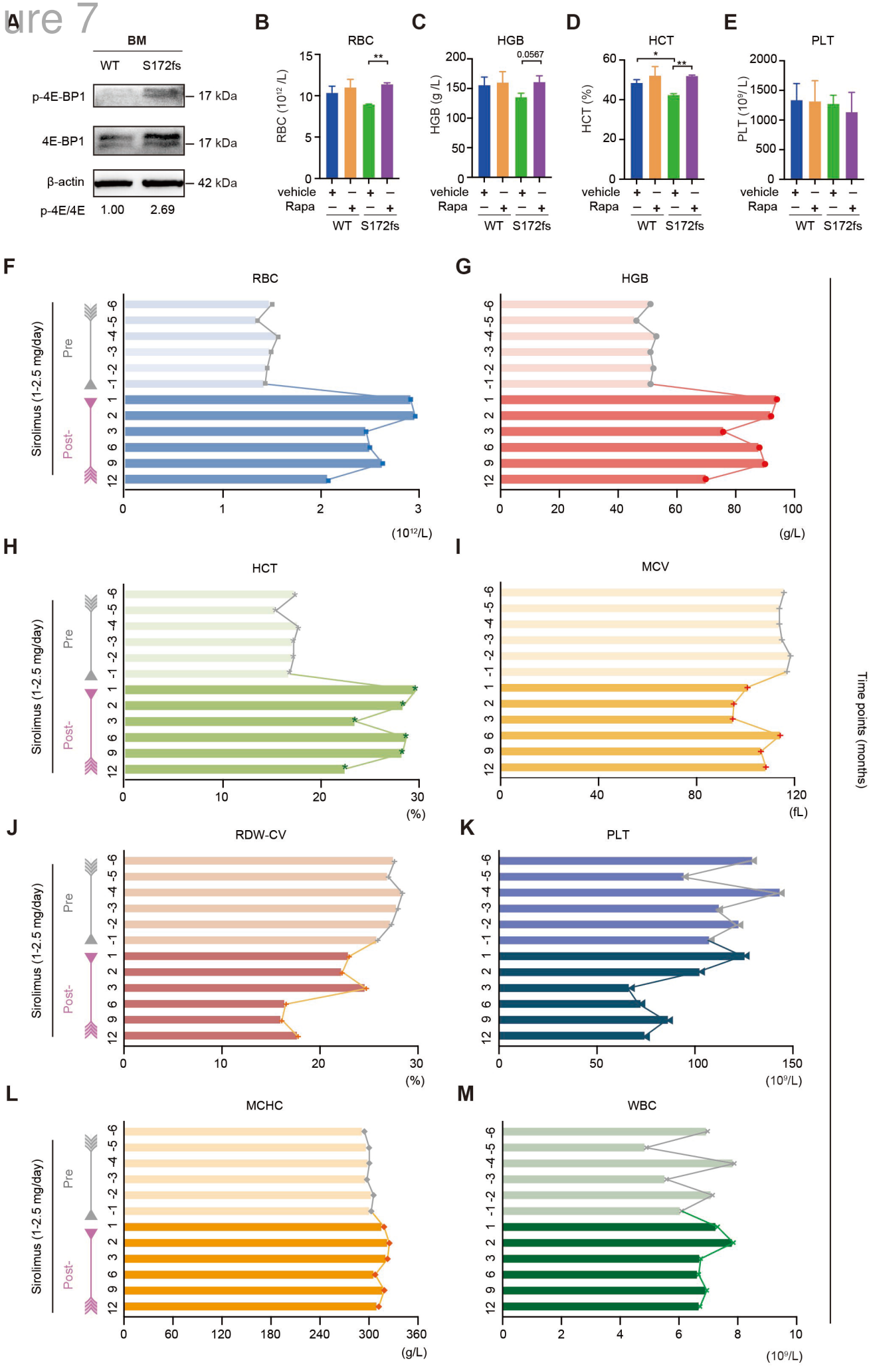

# Alternative Donor Transplantation for Severe Aplastic Anemia (SAA)

## Context of Research

- Stem cell transplantation (SCT) from an HLA-matched sibling donor (MSD) is the standard of care for younger patients with SAA
- When a sibling donor is not available, selecting the most appropriate alternative donor becomes a challenge

## Patients and Methods

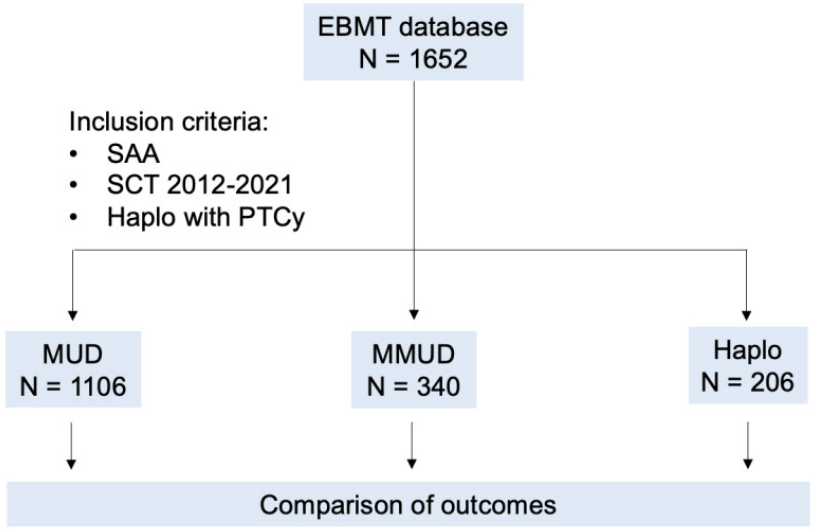


MUD, matched unrelated donor; MMUD, mismatched unrelated donor; Haplo, haploidentical donor

## Main Findings

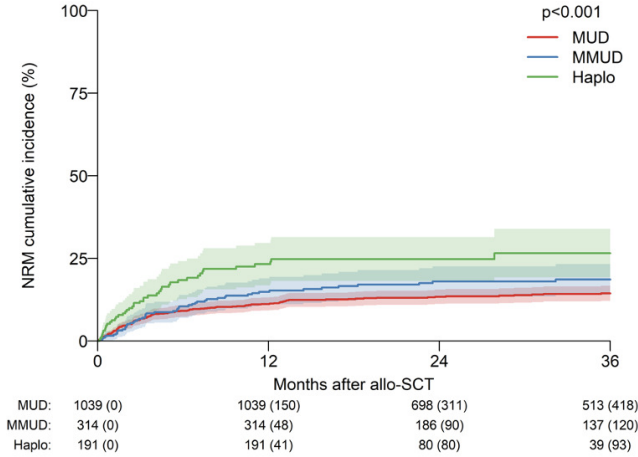


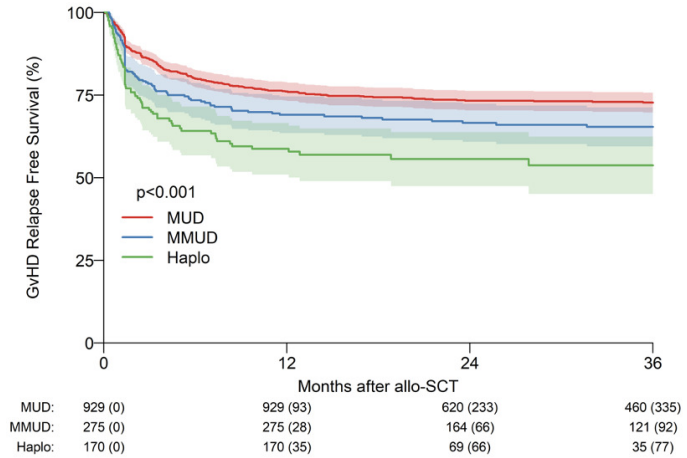


**Conclusions: In patients with SAA who do not have a sibling donor, stem cell transplantation from MUD provides superior survival outcomes compared to both MMUD and Haplo.**

*Montoro et al. DOI: 10.xxxx/**blood**.2024xxxxxx*



**Blood Visual Abstract**